Synthesis and Characterization of Self-Assembled Monolayer and Bilayer Carboxyl-Group Functionalized Magnetic Nanoparticles

L. Li[1], K. Y. Mak[1], C. W. Leung[2], K. Y. Chan[3], W. K. Chan[3], W. Zhong[4], and P. W. T. Pong[1]

[1]Department of Electrical and Electronic Engineering, The University of Hong Kong, Hong Kong
[2]Department of Applied Physics, Hong Kong Polytechnic University, Hong Kong
[3]Department of Chemistry, The University of Hong Kong, Hong Kong
[4]Department of Physics Nanjing University, Nanjing 210093, China

Magnetic nanoparticles functionalized with carboxyl-group have considerable potential to be used as bio-labels due to their conjugation abilities with proteins. Here, we synthesized the iron oxide nanoparticles functionalized with carboxyl groups through self-assembled monolayer coating using citric acid and self-assembled bilayer coating using fatty acids. Their dimension, hydrodynamic size, surface property, and magnetic behavior were characterized through transmission electron microscopy, dynamic light scattering, Fourier transform infrared spectroscopy, thermal gravimetric analysis, and vibrating sample magnetometry. We also confirmed the binding ability of these nanoparticles with bovine serum albumin on thin gold film.

***Index Terms*—Citric acid, fatty acid, magnetic nanoparticle, self-assembled.**

I. Introduction

MAGNETIC bio-detection utilizing magnetoresistance sensors and magnetic nanoparticles possesses great potential for diagnosis and early detection of human diseases. Magnetic nanoparticles are used as bio-probes, and iron oxide nanoparticles (IONPs) have emerged as an excellent candidate due to its biocompatibility [1]. The suitable physicochemical properties of the IONPs, such as the size, magnetic moment, and surface functionality are strictly required for the success of magnetic bio-detection. To acquire ultrahigh bio-detection sensitivity by using magnetoresistive biosensors, such as the detection of single biomolecule with giant magnetoresistance sensors, the size of magnetic bio-labels should be comparable to that of the conjugating biomolecules [2]. The IONPs should be super-paramagnetic with high magnetic moment so that particle agglomeration can be avoided while the IONPS can be detected by magnetic sensors. To ensure their colloidal stabilization in aqueous medium and to conjugate with biologically active agents, magnetic nanoparticles usually bear functional groups on their surfaces, such as carboxyl or amino groups. It is thus worthwhile to find or develop a facile and reliable method for synthesis of the IONPs to meet these requirements.

The synthesis methods of the IONPs are widely discussed in literature [3], [4]. Coprecipitation is a widely used direct synthesis method of water-dispersible IONPs. The main challenge associated with this method is to avoid the aggregation of IONPs products. Self-assembled layer as a technique to control the physical and chemical properties of the surfaces has been paid lots of attention in variety of fields ranging from biology to materials science [5], [6]. It is also an efficient way to functionalize the surfaces of IONPs to well dispersion in aqueous environment.

Here we synthesized carboxyl-group functionalized IONPs through coprecipitation process followed by self-assembled monolayer (SAM) coating using citric acid surfactant and self-assembled bilayer (SAB) coating with fatty acids. This method is simple and straightforward without involving complicated experimental setup. Then we investigated the influence of the carboxylic acid-terminated monolayer and bilayer surface coating on the properties of the IONPs. Since the gold thin film is often used as bio-sensor surface [7] for adsorbing proteins [8], we also investigated the binding ability of these IONPs conjugated with biological molecules on gold surface.

Manuscript received March 02, 2012; revised April 10, 2012; accepted April 17, 2012. Date of current version October 19, 2012. Corresponding author: P. W. T. Pong (e-mail: ppong@eee.hku.hk).

Color versions of one or more of the figures in this paper are available online at http://ieeexplore.ieee.org.

Digital Object Identifier 10.1109/TMAG.2012.2196504

II. Experiments

A. Materials

Ferric chloride hexahydrate ($FeCl_3 \cdot 6H_2O$, $\geqslant$ 99%), ferrous sulfate heptahydrate ($FeSO_4 \cdot 7H_2O$, $\geqslant$ 99.0%), sodium hydroxide ($\geqslant$98%), citric acid ($\geqslant$98%), lauric acid ($\geqslant$98%), and decanoic acid ($\geqslant$99.5%) were purchased from Sigma-Aldrich (USA). All chemicals were used as received.

B. Synthesis of SAM and SAB Carboxyl-Group Functionalized Magnetic Nanoparticles

Our syntheses were based on coprecipitation method followed by coating with self-assembled monolayer (SAM) or self-assembled bilayer (SAB) [6], [9]. Citric acid, decanoic acid, and lauric acid were applied as surfactants. The schematic illustrations of the synthesis procedures are shown in Fig. 1. Three kinds of magnetic nanoparticles with carboxyl-group were fabricated, including IONPs coated with monolayer of citric acid (CA-IONPs), IONPs coated with a bilayer of decanoic acid as the primary surfactant and lauric acid as the secondary surfactant (DALA-IONPs), and IONPs coated with a bilayer of lauric acid as primary surfactant and decanoic acid as second surfactant (LADA-IONPs). In a typical procedure to fabricate IONPs with bilayer coating, the fresh uncoated IONPs synthesized through coprecipitation were dispersed in DI water. 0.3 mmol/ml fatty acid as the first surfactant in water was added under vigorous stirring for 30 minutes at 70°C. The synthesized suspension was precipitated with acetone, and washed with acetone and DI water. The fresh monolayer coated nanoparticles were then combined with DI water and heated to 70°C under vigorous stirring. Solution of fatty acid

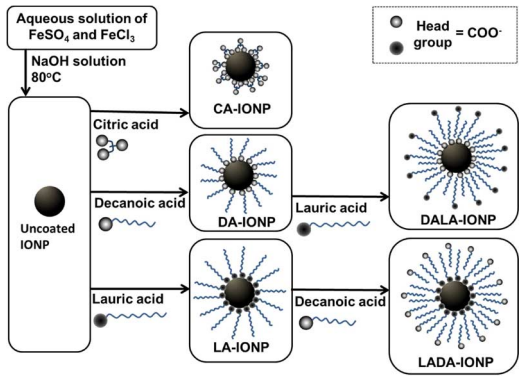

Fig. 1. Schematic representation for the synthesis of self-assembled monolayer (SAM) coating with citric acid and self-assembled bilayer (SAB) coatings with fatty acids to produce magnetic nanoparticles functionalized with carboxyl -group.

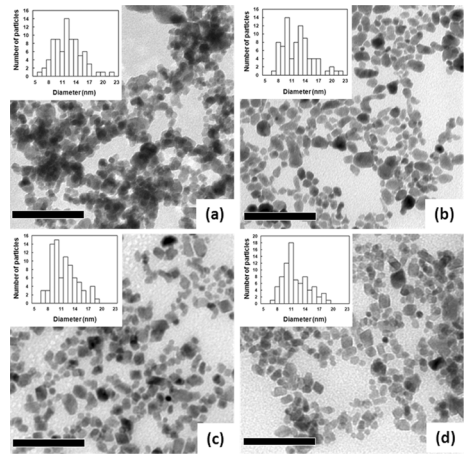

Fig. 2. TEM images of (a) uncoated IONPs, (b) CA-IONPs, (c) DALA-IONPs, and (d) LADA-IONPs. Scale bar, 100 nm. The insets show the histogram of the particles sizes.

as the second surfactant and sodium hydroxide (molar ratio 1:1) in water was added to slurry until the slurry changed into a stable suspension. No phase separation was observed when the suspension was exposed to a 2000 G magnetic field for at least 10 min. For comparison, we also synthesized uncoated IONPs, IONPs coated with monolayer of decanoic acid (DA-IONPs), and IONPs coated with monolayer of lauric acid (LA-IONPs).

C. Characterization of the IONPs

The size and morphology of the IONPs were observed by transmission electron microscopy (TEM, Philips CM100). To prepare the nanoparticle samples, dilute drops of suspension were allowed to dry slowly on carbon-coated copper grids. The Fourier transform infrared (FT-IR) spectra were obtained with a Shimadzu FTIR-8300 spectrometer using KBr pellets. The hydrodynamic size of the IONPs were measured by dynamic light scattering (DLS) using a Malvern Zetasizer 3000 (Malvern, UK). The magnetic property measurement of the samples was carried out at room temperature by using a vibrating sample magnetometer (Lakeshore, VSM 7400). The lyophilized powder samples were immobilized onto two-sided adhesive tape to suppress their Brownian motion. The tape was then rolled up and mounted to the standard sample stud. The magnetization was measured over a range of applied field from $-12\ 000$ to 12 000 Oe. The iron oxide composition was determined by using thermal gravimetric analysis (TGA, Perkin-Elmer TGA-7). The mass loss from 5–10 mg of lyophilized sample was monitored under N_2 at temperatures from 50°C to 600°C at a rate of 50°C/min.

D. Investigation of the Binding Ability of the IONPs Coated With Carboxyl-Group With Protein on Gold Surfaces

To investigate the binding ability of the three synthesized IONPs coated with carboxyl-group (CA-IONPs, DALA-IONPs, and LADA-IONPs) with biological molecules, the experimental process for each IONP sample was based on a procedure reported by Monroe *et al.* [10]. In brief, two silicon wafers with a 200 nm thick gold film on their top were prepared as substrates. One of the wafers was further coated with bovine serum albumin (BSA) through the physical adsorption of protein to the gold surface [8]. After adding the IONP sample (1 mg/ml) onto the wafer surfaces, the binding between the IONPs and BSA could be achieved through the conjugation of carboxyl groups of the IONPs to amino groups of the protein via 1-ethyl-3-(3-dimethylaminopropyl) carbodiimide hydrochloride (EDC)/N-hydroxysuccinimide (NHS) coupling chemistry [11], [12]. In our experiment, 100 μl of EDC/NHS solution (2 mg/ml EDC, 1 mg/ml NHS) was used to activate the carboxyl groups on 1 mg IONP sample, and then the activated carboxyl groups on IONPs conjugated with the amino-containing BSA through an amide bond. After overnight reaction at 4°C, the two wafers were washed by DI water to remove unbound IONPs. A scanning electron microscope (SEM, Hitachi S4800 FEG) with energy dispersive spectrometry (EDS) was used to determine the presence of IONPs on the BSA-pretreated gold surface and the non-BSA-pretreated gold surface. The uncoated IONPs were used to serve as a control.

III. Results and Discussion

Fig. 2 shows TEM images for the uncoated IONPs, CA-IONPS, DALA-IONPS, and LADA-IONPs. Most of the nanoparticles are spherical. We determined the size distribution for each sample by manually measuring the diameters of the nanoparticles from their TEM images (insets in Fig. 2). The iron oxide cores of all the samples show an average size of around 11 nm with a narrow size distribution. The hydrodynamic diameters of these nanoparticles in DI water and in phosphate buffered saline $(\mathrm{PBS},\ \mathrm{pH}\ =\ 7.4)$ as measured by DLS are given in Table I. The average hydrodynamic sizes of the CA-IONPS, DALA-IONPS, and LADA-IONPs in water were about 20–30 nm. This indicates these three kinds of IONPs with carboxyl groups show well-dispersion in water. The average hydrodynamic size of the CA-IONPs, DALA-IONPS, and LADA-IONPs in PBS was determined to be around 20 nm, 1184 nm and 1485 nm, respectively. The uncoated IONPs aggregated into large clusters in aqueous solution with hydrodynamic sizes of tens of micrometers. The size increase of the DALA-IONPS and LADA-IONPs in PBS compared to in water can be attributed to the influence from the salinity and ionic strength in PBS. It was reported that the self-assembled fatty acid vesicles were unstable in sodium chloride at high concentration [13]. The bilayer of

TABLE I
HYDRODYNAMIC SIZE OF FERROFUILD NANOPARTICLES

Samples	D_{TEM} (nm)	D_{DLS_W} (nm) [a]	D_{DLS_P} (nm) [b]
CA -IONPs	11.9 ± 3.3	20.1 ± 13.2	19.5 ± 7.5
DALA -IONPs	11.1 ± 2.8	22.9 ± 4.2	1183.7± 640.5
LADA -IONPs	11.5 ± 2.8	29.8 ± 13.7	1484.7 ± 683.5

[a] D_{DLS_W} – hydrodynamic size of the sample in DI water
[b] D_{DLS_P} – hydrodynamic size of the sample in PBS (pH =7.4)

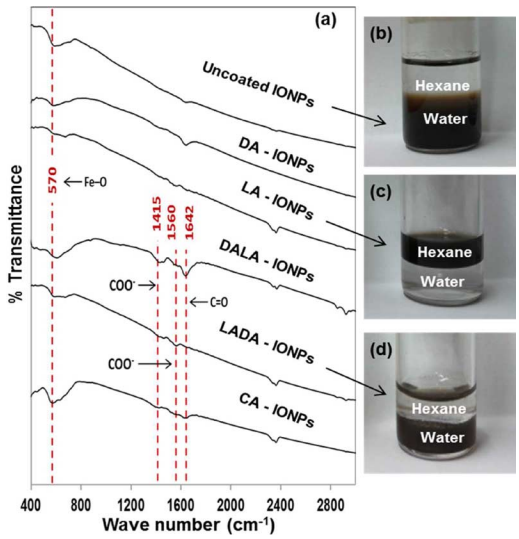

Fig. 3. (a) FT-IR spectra of iron oxide nanoparticles with no coating (uncoated IONPs), monolayer coating (CA-IONPs, LA-IONPs, and DA-IONPs), and bilayer coating (DALA-IONPs and LADA-IONPs). (b), (c), and (d) pictures showing the (b) hydrophilic nature of uncoated IONPs, (c) hydrophobic nature of LA-IONPs, and (d) hydrophilic nature of LADA-IONPs.

the DALA-IONPS and LADA-IONPs in PBS might not be as stable as in water, thus some of them aggregated together and formed clusters with large hydrodynamic sizes. However, since no precipitate was observed in our experiment and their hydrodynamic sizes did not increase as time extended, the DALA-IONPs and LADA-IONPs samples in PBS could still be considered to be stable colloidal solution.

The surface functionalization of the IONPs was analyzed by FT-IR. Fig. 3(a) shows the typical FT-IR spectrum of the IONP samples. The peaks at around 570 cm $^{-1}$ indicates the presence of iron oxide skeleton in all the samples. The bands between 1300 cm^{-1} and 1700 cm^{-1}, representing the carboxylate (COO^-) stretching, were found in the IONPs samples with OA, DALA and LADA coating. The presence of these bands is an evidence of carboxyl-group coating formation around the IONPs. The photos in Fig. 3(b)–(d) displayed the SAB formation process by using lauric acid as primary surfactant and decanoic acid as secondary surfactant on our IONPs. The hydrophilic nature of uncoated IONPs synthesized through coprecipitation method can be observed in Fig. 3(b) where the uncoated IONPS exist only in the water. After the IONPs coated with primary surfactant using lauric acid, LA-IONPs with a hydrophobic nature were dispersed in hexane, and flocculated as the suspension after water was added as shown in Fig. 3(c). When the LA-IONPs were further coated with a second surfactant using decanoic acid, the bilayer formation was induced around the IONPs in aqueous solution because

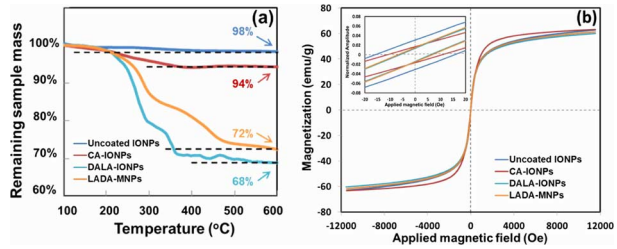

Fig. 4. TGA results and VSM results of synthesized IONPs with no coating, monolayer coating, and bilayer coating. (a) Heating curve of uncoated IONPs, CA-IONPs, DALA-IONPs, and LADA-IONPs was measured by TGA. (b) Magnetization curve of uncoated IONPs, CA-IONPs, DALA-IONPs, and LADA-IONPs was measured by VSM. Inset in (b): Magnified views of hysteresis loop in low magnetic field. [See the electronic version of the Journal for a color version of this figure.]

water is a poor solvent for both hydrophobic domains of added fatty acid and the hydrophobic LA-coated IONPs. Thus the LADA-IONPs were formed and transferred into an aqueous phase [Fig. 3(d)]. In this experiment, the DA-IONPs and DALA-IONPs showed similar behavior as LA-IONPs and LADA-IONPs, respectively. So we can confirm that the bilayer of fatty acids is indeed formed around the IONPs surface.

The heating curve and magnetic hysteresis curve of the nanoparticles were measured by TGA and VSM, as shown in Fig. 4. The weight percentage of iron oxide core in CA-IONPs, DALA-IONPs, and LADA-IONPs samples was about 94%, 72% and 68%, as determined by TGA [Fig. 4(a)]. The saturation magnetization (Ms) for iron oxide cores of uncoated IONPs, CA-IONPs, DALA-IONPs, and LADA-IONPs are 63, 63, 60, and 62 emu/g, respectively [Fig. 4(b)]. They are less than the Ms for bulk Fe_3O_4 (92 emu/g) and the Ms for bulk γ-Fe_2O_3(74 emu/g) [14], and are comparable to the Ms reported for the magnetite nanoparticles with sizes around 10 nm [15]. The magnified views of the major loops normalized by the maximum magnetization in the low magnetic field are shown in the inset of Fig. 4(b). The low ratio of remanant magnetization to saturation magnetization (Mr/Ms $\approx$ 0.01) indicates those samples display a superparamagnetic behavior. The coercivity of the CA-IONPs (11 Oe) and fatty-acid bilayer coated IONPs (6$\sim$7 Oe) was found to be lower than the uncoated IONPs (16 Oe). The reason might be because the monolayer coating and bilayer coating surrounding the IONPs increase the distance between the nanoparticles compared to the uncoated IONPs. It is reported that when the distance between the nanoparticles increases, the interparticle dipole-dipole interaction reduces and thus their coercivity becomes smaller [16].

The experiment to determine the biologically binding ability of the carboxyl-group functionalized IONPs samples was carried out with the BSA-pretreated gold surface and the non-BSA-pretreated gold surface through a standard EDC/NHS chemical coupling method. Fig. 5 presents the EDS results of the gold surfaces after the treatment of LADA-IONPs, the insets were corresponding SEM images. In the control experiment, no iron was found on the gold surface precoated with BSA after treatment with uncoated IONPs [Fig. 5(a)], which indicates the uncoated IONPs did not display binding ability to BSA-pretreated gold surface. The aggregates shown in the SEM image

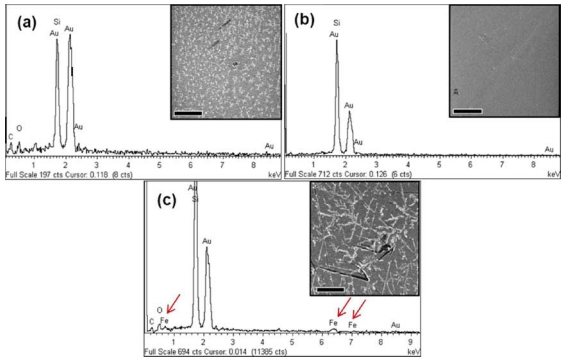

Fig. 5. Elemental EDS analysis of (a) BSA-pretreated gold surface after treatment of uncoated IONPs, (b) Non-BSA-pretreated gold surface and (c) BSA-pretreated gold surface after the treatment of LADA-IONPs. The presence of iron was indicated by red arrows in (c). Inset shows the SEM images of respective gold surface that were analyzed using EDS. Scale bar, 50 μm.

TABLE II
PRESENCE OF THE ELEMENTS ON GOLD SURFACES AFTER TREATMENT WITH IONPS SAMPLES

Gold surface	IONPs sample	Presence of elements (EDS) [a]
Non-BSA-pretreated	Uncoated-IONPs	Si, Au
Non-BSA-pretreated	CA-IONPs	Si, Au
Non-BSA-pretreated	DALA-IONPs	Si, Au
Non-BSA-pretreated	LADA-IONPs	Si, Au
BSA-pretreated	Uncoated-IONPs	Si, Au , O, C
BSA-pretreated	CA-IONPs	Si, Au , O, C, Fe
BSA-pretreated	DALA-IONPs	Si, Au , O, C, Fe
BSA-pretreated	LADA-IONPs	Si, Au , O, C, Fe

[a] Si = silicon, Au = gold, O = oxygen, C = carbon, Fe = iron.

[inset in Fig. 5(a)] were due to the BSA coated on the gold surface. For the non-BSA-pretreated gold surface [Fig. 5(b)] and the BSA-pretreated gold surface [Fig. 5(c)] after treatment with LADA-IONPs, the presence of iron was only found on the BSA-pretreated gold surface [indicated by red arrow in Fig. 5(c)]. This indicates the LADA-IONPs showed binding ability onto the BSA-pretreated gold surface, but not onto the non-BSA-pretreated gold surface. Since the uncoated IONPs sample was not able to bind with BSA-pretreated gold surface, the binding ability of LADA-IONPs onto the BSA-pretreated gold surface should be through the carboxyl-group of the LADA-IONPs to the amino-group of the BSA via EDC/NHS coupling. The aggregates shown in the SEM image [inset in Fig. 5(c)] should be the LADA-IONPs-BSA complexes. The principle elements in the complexes were confirmed by the presence of iron, carbon, and oxygen in the EDS result [Fig. 5(c)].

Table II shows the final presence of the elements determined by EDS on non-BSA-pretreated and BSA-pretreated gold surface after the reaction with IONPs samples in all the experiments (one kind of IONPs sample was used in one experiment). After the treatment with CA-IONPs, DALA-IONPS, and LADA-IONPs, we observed the presence of elements of Si and Au on the non-BSA-pretreated gold surface, and elements of Si, Au, O, C, and Fe on the BSA-pretreated gold surface. Elements of Si and Au were from the silicon substrate sputtered with thin gold film. Elements of O, C and Fe are the principle elements in the IONPs-BSA complexes. Similar to our discussion about the binding ability of LADA-IONPs with BSA, these EDS results confirmed the binding ability of CA-IONPs and DALA-IONPs with BSA.

IV. CONCLUSION

We fabricated the carboxyl-group functionalized IONPs coated with monolayer of citric acid, and IONPs coated with bilayer of fatty acids. The influence of the coating material on the dimensions, aqueous stability, and magnetic properties of IONPs was revealed. In conclusion, these three kinds of synthesized IONPs samples with carboxyl-group (CA-IONPs, DALA-IONPs and LADA-IONPs) exhibited the core sizes around 11 nm, well-dispersion in aqueous solution, and sufficient iron oxide core saturation magnetization above 60 emu/g. Further, the presence of carboxylic group provides an avenue to establish bond formation with proteins and other molecules. We have shown these particles can bind with BSA by standard procedure. The research results demonstrate that coprecipitation with SAB and SAM is a feasible alternative for manufacturing functionalized magnetic nanoparticles suitable to facilitate biological labeling.

ACKNOWLEDGMENT

This work was supported by the Seed funding Program for Basic Research from the University of Hong Kong and the RGC-GRF grant (HKU 7049/11P). Assistance from Frankie Chan (EMU, HKU) on TEM examination is gratefully acknowledged.

REFERENCES

[1] S. I. Park, J. H. Lim, J. H. Kim, H. I. Yun, and C. O. Kim, *J. Magn. Magn. Mater.*, vol. 304, pp. e406–e408, 2006.
[2] G. Li, S. Sun, R. J. Wilson, R. L. White, N. Pourmand, and S. X. Wang, *Sens. Actuators A, Phys.*, vol. 126, pp. 98–106, 2006.
[3] A. Goodarzi, Y. Sahoo, M. Swihart, and P. Prasad, in *Mater. Res. Soc. Symp. Proc.*, 2004, vol. 789, no. 6.6.
[4] P. Guardia, N. Pérez, A. Labarta, and X. Batlle, *Langmuir*, vol. 26, pp. 5843–5847, 2009.
[5] P. L. Luisi and P. Stano, *The Minimal Cell: The Biophysics of Cell Compartment and the Origin of Cell Functionality*. New York: Springer-Verlag, 2010.
[6] S. I. Park, J. H. Lim, J. H. Kim, H. I. Yun, J. S. Roh, C. G. Kim, and C. O. Kim, *Physica Status Solidi (b)*, vol. 241, pp. 1662–1664, 2004.
[7] R. L. Edelstein, C. R. Tamanaha, P. E. Sheehan, M. M. Miller, D. R. Baselt, L. J. Whitman, and R. J. Colton, *Biosens. Bioelectron.*, vol. 14, pp. 805–813, 2000.
[8] C. S. S. R. Kumar, *Nanocomposites*. Hoboken, NJ: Wiley, 2010.
[9] S. Nigam, K. Barick, and D. Bahadur, *J. Magn. Magn. Mater.*, vol. 323, pp. 237–243, 2011.
[10] B. G. Nidumolu, M. C. Urbina, J. Hormes, C. S. S. R. Kumar, and W. T. Monroe, *Biotechnol. Prog.*, vol. 22, pp. 91–95, 2006.
[11] K. D. Wittrup and G. L. Verdine, *Protein Engineering for Therapeutics*. New York: Elsevier, 2012.
[12] G. T. Hermanson, *Bioconjugate Techniques*. New York: Academic, 2008.
[13] J. P. Jolivet, É. Tronc, and C. Chanéac, *Comptes Rendus Chimie*, vol. 5, pp. 659–664, 2002.
[14] T. Yogo, T. Nakamura, W. Sakamoto, and S. Hirano, *J. Mater. Res.*, vol. 15, pp. 2114–2120, 2000.
[15] M. Morales, T. K. Jain, V. Labhasetwar, and D. Leslie-Pelecky, *J. Appl. Phys.*, vol. 97, p. 10Q905, 2005.
[16] A. Tomitaka, T. Koshi, S. Hatsugai, T. Yamada, and Y. Takemura, *J. Magn. Magn. Mater.*, vol. 323, pp. 1398–1403, 2011.